RSC Advances

PAPER

View Article Online
View Journal | View Issue

Cite this: *RSC Adv.*, 2017, **7**, 8082

Centrosymmetric to noncentrosymmetric structural transformation of new quaternary selenides induced by isolated dimeric [Sn_2Se_4] units: from $Ba_8Ga_2Sn_7Se_{18}$ to $Ba_{10}Ga_2Sn_9Se_{22}$†

Yan-Yan Li,[a] Jin-Qiu Wang,[ac] Peng-Fei Liu,[ac] Hua Lin,[a] Ling Chen[ab] and Li-Ming Wu*[ab]

Received 24th November 2016
Accepted 18th January 2017

DOI: 10.1039/c6ra27253c

www.rsc.org/advances

A noncentrosymmetric structure is a prerequisite of many important properties, such as ferroelectric, piezoelectric and nonlinear optical properties. The design synthesis of a noncentrosymmetric compound is highly desired but it is a great challenge. Herein, two new quaternary selenides, $Ba_8Ga_2Sn_7Se_{18}$, **1** and $Ba_{10}Ga_2Sn_9Se_{22}$, **2**, have been discovered by solid-state reactions. Compound **1** crystallizes in the centrosymmetric space group *Pnma* (no. 62) with a = 12.466 (9) Å, b = 9.358 (6) Å, c = 18.14 (2) Å, V = 2116 (3) Å^3, Z = 2; and **2** crystallizes in the noncentrosymmetric space group $Cmc2_1$ (no. 36) with a = 9.384 (2) Å, b = 44.834 (6) Å, c = 12.416 (2) Å, V = 5224 (2) Å^3, Z = 4. The major motif of both **1** and **2** is the $[Ga_2Sn_7Se_{18}]_\infty^{16-}$ ladder chain built by alternately jointed $GaSe_4$ tetrahedra and $SnSe_4$ tetragonal pyramids, and to each of these polyhedra, an accessory ($SnSe_3$ pyramid or Sn_2Se_4 dimer) is attached. Interestingly, the noncentrosymmetric structure of **2** is the combination of centrosymmetric **1** and the imbedded isolated dimeric [Sn_2Se_4] with a C_{2v} polar symmetry that separates every two such ladder chains. **1** and **2** directly illustrate that a simple combination reaction can drive the centrosymmetric to noncentrosymmetric structural transformation.

Introduction

Chalcogenides play important roles in many fields owing to their fascinating structural complexity and remarkable properties, such as infrared nonlinear optical (NLO), thermoelectric, and magnetic properties.[1–7] Among them, noncentrosymmetric chalcogenides are of special interest, because the noncentrosymmetric structure is a prerequisite for ferroelectric, piezoelectric and NLO properties.[8–17] We realize that a slight component variation of a centrosymmetric chalcogenide, *via* element substitution or stoichiometry tuning, may lead to a structural transformation into a noncentrosymmetric one, as observed in particular in some low-dimensional chalcogenides. For example, adding a secondary building unit SbS_3 pyramid (SbS_3 : GaS_4 = 1 : 4) into the centrosymmetric $Ba_5Ga_2S_8$, which helped to disconnect the isolated GaS_4 tetrahedron array in breaking the symmetry of the inversion center, led to an 0D noncentrosymmetric compound $Ba_{23}Ga_8Sb_2S_{38}$. And this compound exhibited very large second harmonic generation of 22 × $AgGaS_2$ at 2.05 μm.[15] The 0D compounds $Ba_3(BS_3)_{1.5}(SbS_3)_{0.5}$ and $Ba_3(BS_3)(SbS_3)$ merely differing in the ratio of BS_3/SbS_3 show an interesting centrosymmetric-to-noncentrosymmetric structural relationship.[16] Geng *et al.* utilized gallium or indium and obtained a centrosymmetric Ba_2BiGaS_5, and a noncentrosymmetric Ba_2BiInS_5 (ref. 17) with different alignment of BiS_5 tetragonal pyramids and neighboring MS_4 (M = Ga, In) tetrahedra. Besides, different Ln cations lead to different crystal symmetries, like: controsymmetric $Ba_2LnGaTe_5$ (Ln = Sm or Gd) and noncentrosymmetric $Ba_2LnGaTe_5$ (Ln = Dy, Er, Y).[18]

The family A/Ga/Sn/Q (A = alkaline-earth metal; Q = S, Se, Te) attracts our attention. One reason is that the asymmetric GaQ_n units are able to build many noncentrosymmetric compounds, such as $BaGa_4Q_7$ (Q = S, Se),[19] $BaGa_2GeQ_6$ (Q = S, Se),[20] $Ba_{23}Ga_8Sb_2S_{38}$,[15] $Li_2Ga_2GeS_6$,[21] $ACd_4Ga_5S_{12}$ (A = K, Rb, Cs),[22] $Ba_2Ga_8MS_{16}$ (M = Si, Ge),[23] and Ln_4GaSbS_9 (Ln = Pr, Nd, Sm, Gd–Ho).[24] Another reason is that Sn^{2+} possessing active lone pair electrons tends to adopt polar local coordinations, *e.g.*, $Sn^{2+}Q_4$ tetragonal pyramid in $SnGa_4Q_7$ (Q = S, Se),[25] $Sn^{2+}S_3$ pyramid in $Ba_8Sn_4S_{15}$,[26] and $(Sn^{2+})_2S_3$ trigonal bipyramid in $Ba_7Sn_5S_{15}$.[27] In these

[a]*Key Laboratory of Optoelectronic Materials Chemistry and Physics, Fujian Institute of Research on the Structure of Matter, Chinese Academy of Sciences, Fuzhou, Fujian 350002, People's Republic of China. E-mail: liming_wu@fjirsm.ac.cn; Fax: +86 10 6220 9119; Tel: +86 10 6220 9980*

[b]*Key Laboratory of Theoretical and Computational Photochemistry of Ministry of Education, Department of Chemistry, Beijing Normal University, Xin-wai-da-jie No.19, Beijing, 100875, People's Republic of China*

[c]*University of Chinese Academy of Sciences, Beijing 100039, People's Republic of China*

† Electronic supplementary information (ESI) available. CCDC 1475011 and 1475012. For ESI and crystallographic data in CIF or other electronic format see DOI: 10.1039/c6ra27253c

compounds, Sn^{2+} plays the leading role in the SHG. However, up to now, only three compounds containing Sn^{4+} in the A/Ga/Sn/Q family are known: noncentrosymmetric $Ba_4Ga_4SnSe_{12}$ and $BaGa_2SnSe_6$, and centrosymmetric $Ba_6Ga_2SnSe_{11}$.[28,29] Members containing low oxidation state Sn^{2+} or mixed oxidation states (Sn^{2+} and Sn^{4+}) are still rare.

Herein, two new selenides, centrosymmetric $Ba_8Ga_2Sn_7Se_{18}$, **1** and noncentrosymmetric $Ba_{10}Ga_2Sn_9Se_{22}$, **2**, are discovered. For the first time, **1** and **2** illustrate an interesting and direct structure transformation from centrosymmetric to noncentrosymmetric. The structure of **2** can be regarded as a composition of structure of **1** with an asymmetric matrix of the isolated dimeric $[Sn_2Se_4]$. Syntheses, crystal structures, electronic structures and DFT studies are also reported.

Experimental section

Synthesis

The reagents were used as obtained: Ba rod (Alfa Aesar China (Tianjin) Co., Ltd., 99.9%), Ga shot, Sn grain, and Se powder (Sinopharm Chemical Reagent Co., Ltd., 99.999%). And one single piece of the barium rod was used as the starting reactant. The binary compounds BaSe and SnSe were synthesized at 850 °C by elemental mixture in sealed silica tubes under vacuum of 10^{-2} Pa. And the binary Ga_2Se_3 was synthesized at 680 °C by a boron-chalcogen method.[30–34]

$Ba_8Ga_2Sn_7Se_{18}$, 1. The black block-shaped crystals of **1** were first discovered by a reaction of elements of Ba, Ga, Sn, and Se in a 7 : 2 : 3 : 14 molar ratio with a total weight of 400 mg. The reactants were loaded into a graphite crucible, and sealed in an evacuated silica tube under 10^{-2} Pa atmosphere, and then heated to 980 °C within 50 h and kept there for 48 h, then cooled to 400 °C at a rate of 5 °C h^{-1}.

Many efforts revealed that such stoichiometric reactions could not produce pure phase. Instead, black crystals of **1**, and $Ba_6Sn_6Se_{13}$ (ref. 35) as a secondary phase together with few red crystals of $Ba_5Ga_2Se_8$ (ref. 36) were produced. We considered the reason might be the insufficient contact/mixing between Ga and the other reactants. Therefore, binary BaSe, Ga_2Se_3 and SnSe were used instead. The mixture of BaSe, Ga_2Se_3 and SnSe in a molar ratio of 8 : 1 : 7 with a total weight of about 500 mg was ground carefully and pressed into a pellet. Then the pellet was put into a graphite crucible in an evacuated silica jacket, and subsequently heated to 750 °C in 34 h, kept for 80 h, and then cooled to 300 °C within 100 h before the furnace was turned off. The homogenous **1** was produced according to the XRD pattern as shown in ESI Fig. S1a.†

$Ba_{10}Ga_2Sn_9Se_{22}$, 2. The black block-shaped crystals of **2** were initially obtained from a reaction of Ba, Ga, Sn, and Se elements in a 13 : 2 : 10 : 26 ratio with a total weight of 300 mg. And pure phase **2** was obtained by the reaction of cold-pressed pellet of the well ground mixture of binary BaSe, Ga_2Se_3 and SnSe in a 10 : 1 : 9 ratio with a total weight of about 500 mg. The heating profile was heating to 750 °C in 50 h, dwelling for 80 h, then cooling to 300 °C at a rate of 4 °C h^{-1}. The XRD pattern showed the homogeneity of the product (ESI Fig. S1b†). The crystals of **2** were relatively moisture sensitive.

Single-crystal X-ray crystallography

The single crystal diffraction data were collected on a Mercury CCD equipped with graphite-monochromated Mo Kα radiation (λ = 0.71073 Å) at 293 K. The data were corrected for Lorentz and polarization factors. And the structures were solved by the direct methods and refined by the full-matrix least-squares fitting on F^2 using the SHELX-97.[37]

The single-crystal X-ray diffraction data revealed two sets of new unit cell parameters of a = 12.5 Å, b = 9.4 Å, c = 18.1 Å, $\alpha = \beta = \gamma = 90°$ for **1**; and a = 9.4 Å, b = 44.8 Å, c = 12.4 Å, $\alpha = \beta = \gamma = 90°$ for **2** indicating the orthorhombic crystal system. Subsequently, the structure of **1** was solved in the suggested space group of *Pnma* (62) and refined with R_1 = 9.49% and wR_2 = 31.10%. However, an abnormal large atom displacement parameter of Sn(1) ($U_{eq.}$ = 0.093) was seen, such a value was about 3–4 times as those of other Sn sites (Sn(2): 0.031, Sn(3): 0.021, Sn(4): 0.027). Therefore, the occupancy of Sn(1) was allowed to refine freely. The refinement resulted in a reasonable temperature factor of 0.024 and an occupancy of 45.297% for Sn(1), and better R values (R_1 = 0.0408 and wR_2 = 0.0928). The PLATON[38] checking found no missing or higher symmetry elements exiting in **1**. The partial occupancies of Sn were also found in compound $BaAu_2SnS_4$.[39] To keep the charge balance, the occupancy of Sn(1) was fixed to 0.5. Consequently, the final R values were converged to R_1 = 0.0415 and wR_2 = 0.920 (Table 1, ESI Table S1a†). The final charge-balanced formula was established as $(Ba^{2+})_8(Ga^{3+})_2(Sn^{2+})_7(Se^{2-})_{18}$. Meanwhile, all the subgroups of *Pnma* were checking. For instance, similar refinement of **1** in $Pna2_1$ generated higher R values of R_1 = 0.0429 and wR_2 = 0.1275. And the subsequent checking with PLATON suggested the space group *Pnma*. Other subgroups of *Pnma*, such as $Pmn2_1$, $Pmc2_1$, and $P2_12_12_1$, gave similar results, and none of them generated reasonable bond lengths and atomic displacement parameters. Therefore, the structure solved in *Pnma* (62) space group was sound.

Table 1 Crystal data and structure refinements of $Ba_8Ga_2Sn_7Se_{18}$, **1** and $Ba_{10}Ga_2Sn_9Se_{22}$, **2**

Formula	$Ba_8Ga_2Sn_7Se_{18}$	$Ba_{10}Ga_2Sn_9Se_{22}$
fw	3490.27	4318.17
Crystal system	Orthorhombic	Orthorhombic
Crystal colour	Black	Black
Space group	*Pnma*	$Cmc2_1$
a (Å)	12.466 (9)	9.384 (2)
b (Å)	9.358 (6)	44.834 (6)
c (Å)	18.14 (2)	12.416 (2)
V (Å^3)	2116 (3)	5224 (2)
Z	2	4
D_c (g cm^{-3})	5.5	5.1
μ (mm^{-1})	28.1	24.1
GOOF on F^2	1.137	0.981
R_1, wR_2 ($I > 2\sigma(I)$)[a]	0.0415, 0.0920	0.0418, 0.0873
R_1, wR_2 (all data)	0.0490, 0.0959	0.0480, 0.0897
Flack parameter	N/A	0.00 (3)
Largest diff. peak and hole (e Å^{-3})	2.19/−1.77	1.99/−2.13

[a] $R_1 = \sum||F_o| - |F_c||/\sum|F_o|$ for $F_o^2 > 2\sigma(F_o^2)$; w$R_2 = \sum[w(F_o^2 - F_c^2)]/\sum[w(F_o^2)^2]^{1/2}$.

In case of **2**, the space group of $Cmc2_1$ was first adopted to solve the structure, which generated good R values ($R_1 = 0.0663$ and $wR_2 = 0.1791$) but relatively large isotropic temperature factors for Sn(1) and Sn(5) ($U_{eq.} = 0.090$ and 0.1). Thus, the occupancies of Sn(1) and Sn(5) were allowed to refine freely, which generated comparative temperature factors (0.019 and 0.019), better R values ($R_1 = 0.0417$ and $wR_2 = 0.0888$) and occupancies of 48.64% Sn(1) and 48.64% Sn(5), respectively. Then the occupancies of Sn(1) and Sn(5) were fixed to 0.5, and the final refinement converged to R values of $R_1 = 0.0418$ and $wR_2 = 0.0873$ and a charge-balanced formula of $(Ba^{2+})_{10}(Ga^{3+})_2(Sn^{2+})_9(Se^{2-})_{22}$ (Table 1, ESI Table S1b†). The PLATON checking found no missing or higher symmetry elements exiting in **2**. Selected bond distances and angles are listed in ESI Tables S2 and S3.†

Elemental analyses

The semiquantitative energy dispersive X-ray spectra (EDX, Oxford INCA) were measured on a field emission scanning electron microscope (FESEM, JSM6700F). The quantitative inductively coupled plasma (ICP) emission spectra were recorded with the aid of an Ultima-2 inductively coupled plasma emission spectrometer (ICP-OES). The EDX results confirmed the presence of Ba, Ga, Sn, and Se. And the results of EDX and ICP indicated the ratios of Ba : Ga : Sn : Se in the approximate molar ratio of 8 : 2 : 7 : 18 for **1** and 10 : 2 : 9 : 22 for **2** (ESI Fig. S2, Tables S4, and S5†), which were in accordance with the single crystal diffraction refinements.

Powder X-ray diffraction

The XRD patterns were collected on a Rigaku MiniFlex II diffractometer by using Cu Kα radiation. The scanning range was 10–70° in 2θ with a step size of 0.02°. As shown in ESI Fig. S1,† the experimental XRD patterns of **1** and **2** were in good agreement with the simulated ones based on the single crystal data.

Thermal analyses

Thermogravimetric (TG) analyses of compound **1** and **2** were measured on a NETZSCH STA 449F3 simultaneous analyzer under a constant flow of N_2. The samples were enclosed in an Al_2O_3 crucible, heated from room temperature to 1200 °C at a rate of 20 °C min^{-1}.

Infrared and UV-Vis-near-IR diffuse reflectance spectra

The UV-Vis-near-IR diffuse reflectance spectra were measured at room temperature using a Perkin-Elmer Lambda 950 UV-Vis spectrophotometer equipped with an integrating sphere attachment and $BaSO_4$ as a reference. The absorption spectra were calculated from the reflection spectra according to the Kubelka–Munk function: $\alpha/S = (1 - R)^2/2R$, where α was the absorption coefficient, S was the scattering coefficient, and R was the reflectance.[40] The IR data were measured by a Nicolet Magana 750 FT-IR spectrophotometer in the range of 2.5–25 μm for **2**. Powder sample of **2** was ground with KBr and pressed into a transparent pellet for the measurement.

Powder second harmonic generation (SHG) measurements

The SHG response of compound **2** was performed on a modified Kurtz-NLO system using 1064 nm and 2050 nm laser radiation.[41] The particle size of the sieved sample was 30–46 μm. Single crystal of $AgGaS_2$ (2 cm × 2 cm × 2 cm single crystals from Anhui Institute of Optics and Fine Mechanics Chinese Academy of Sciences) was crushed and then sieved into similar particle size, and this was used as a reference.

Computational section

Utilizing density functional theory (DFT) implemented in the Vienna *ab initio* simulation package code,[42] the electronic structures were investigated. Projector augmented wave (PAW) method[43] were used for the ionic cores and the generalized gradient approximation (GGA) were used for the exchange–correlation potential, in which the Perdew–Burke–Ernzerhof (PBE) type[44] exchange–correlation was adopted. Ba $5s^25p^66s^2$, Ga $4s^24p^1$, Sn $5s^25p^2$, and Se $4s^24p^4$ were treated as valence electrons. The reciprocal space was sampled with 0.05 $Å^{-1}$ spacing in the Monkhorst–Pack scheme for the structure optimization, and denser k-point grids less than 0.02 $Å^{-1}$ spacing were adopted for the property calculation. A mesh cutoff energy of 500 eV was used to determine the self-consistent charge density. All geometries were relaxed until the Hellmann–Feynman force on atoms was less than 0.01 eV $Å^{-1}$ and the total energy change was less than 1.0×10^{-5} eV. The calculation models of **1** and **2** were shown in ESI Fig. S3 and S4.† The structure of the isostructural $BaSnS_2$ (ref. 45) was adopted to simulate the $BaSnSe_2$ structure in the energy calculation of the combination reaction ($Ba_8Ga_2Sn_7Se_{18}$ (**1**) + $2BaSnSe_2$ = $Ba_{10}Ga_2Sn_9Se_{22}$ (**2**)).

Results and discussion

Crystal structure

Crystal structure of $Ba_8Ga_2Sn_7Se_{18}$, 1. Orthorhombic **1** crystallizes in the centrosymmetric *Pnma* (no. 62) with a = 12.466 (9) Å, b = 9.358 (6) Å, c = 18.14 (2) Å and $Z = 2$ (Table 1). There are 2 crystallographically independent Ba atoms, 1 independent Ga atom, 4 independent Sn atoms and 7 independent Se atoms. All Ba atoms, two of the Se atoms are at the Wyckoff 8d sites, and the other atoms occupy the Wyckoff 4c sites. The occupancies of all atoms are 100% except for Sn(1) (50%) (ESI Table S1a†).

As illustrated in Fig. 1a and 2a, the major structure motif of **1** is the infinite 1D $[Ga_2Sn_7Se_{18}]_\infty^{16-}$ ladder chain that is built by alternatively jointed $GaSe_4$ tetrahedron and $SnSe_4$ tetragonal pyramid. To each of such polyhedra, an accessorial $SnSe_3$ (Sn = Sn(2)) pyramid or Sn_2Se_4 (Sn = Sn(3), Sn(4)) dimer is attached *via* a common edge or an apex, respectively. Also such a ladder chain can be viewed as the combination of two single chains jointed by common Se atoms, denoted as Chain 1 and Chain 2 (Fig. 2a). As shown, Chain 1 is operated into Chain 2 through

the center of symmetry. The ladder chain is packed by a sequence of …AA^a… along the *c* direction (Fig. 1a). Note that the *a*-glide plane at (*x*, *y*, 1/4) operates A into A^a.

Selected bond distances are listed in ESI Table S2a.† The Ba atom is 7-fold coordinated in a monocapped trigonal prism with Ba–Se bond lengths ranging from 3.282 (2) to 3.576 (2) Å (ESI Fig. S5†). These lengths are comparable to 3.218 (1)–3.859 (2) Å in Ba_2MLnSe_5 (M = Ga, In; Ln = Y, Nd, Sm, Gd, Dy, Er).[46] The Ga–Se distances range from 2.384 (2) to 2.421 (2) Å, which are comparable to those of 2.364–2.499 Å in $Ba_5Ga_2Se_8$.[36] The 3-fold coordinated Sn atoms (Sn(2), Sn(3), Sn(4)) have Sn–Se bond lengths falling in the normal range of 2.584 (2) to 2.891 (2) Å. The calculated bond valence sums (BVS)[47] for these Sn–Se bonds are 1.903, 1.771, and 2.374, respectively. The BVS values are close to the reported values of Sn^{2+} with 3-fold coordination, *e.g.*, from 2.208 to 2.147 in $Ba_6Sn_6Se_{13}$.[35] Differently, the 4-fold coordinated Sn(1) atom has a site occupancy of 50%, and shows 3 short Sn(1)–Se bonds (2.766 (3), 2.831 (2), and 2.831 (2) Å) and 1 long bond (2.966 (3) Å) (ESI Fig. S6†). The calculated BVS of Sn(1) is 2.025. Hence, the valence state of Sn(1) should be 2+. Similar situations are found in $K_2Sn_4Se_8$,[48] $SrSn_2Se_4$,[49] and $SnGa_4Se_7$,[25] in which the Sn–Se bond lengths are ranging from 2.578 to 3.132 Å. Consequently, in $Ba_8Ga_2Sn_7Se_{18}$, **1**, the oxidation states of Ba, Ga, Sn and Se atoms are assigned to be 2+, 3+, 2+ and 2−.

Crystal structure of $Ba_{10}Ga_2Sn_9Se_{22}$, 2. Orthorhombic **2** crystallizes in the noncentrosymmetric $Cmc2_1$ space group (no. 36) with $a = 9.384$ (2) Å, $b = 44.834$ (6) Å, $c = 12.416$ (2) Å and $Z = 4$ (Table 1). There are 5 crystallographically independent Ba atoms, 2 Ga atoms, 10 Sn and 17 Se atoms. All Ba atoms and five of the Se atoms are sitting at the Wyckoff 8b sites, and the rest of atoms occupy the Wyckoff 4a sites. The occupancies of all atoms are 100% except for Sn(1) (50%) and Sn(5) (50%) (ESI Table S1b†).

Compound **2** is also a ladder chain structure, surprisingly, the ladder chains in **2** are nearly identical to those in **1**. For example, the M–Se bond length and the Se–M–Se bond angle (M = Ga(1), Ga(2); Sn(2)–(4), Sn(6)–(8)) deviate less than 0.4 and 3%, with respect to those in **1** (ESI Tables S2 and S3†). The two short unit cell axes of **1** and **2** are nearly the same, only the long axis is expanded owing to the embedding of $[Sn_2Se_4]$ dimers (Sn = Sn(9), Sn(10)). As shown in Fig. 1b, every two ladder chains are separated at the light blue moiety by the isolated $[Sn_2Se_4]$ dimers. The ladder chain in **2** is also built by alternatively jointed $GaSe_4$ tetrahedra (Ga = Ga(1) and Ga(2)) and $SnSe_4$ tetragonal pyramids (Sn = Sn(1) and Sn(5)). To each of such polyhedra, an accessorial $SnSe_3$ (Sn = Sn(2) or Sn(6)) pyramid or Sn_2Se_4 (Sn = Sn(3), Sn(4) or Sn(7), Sn(8)) dimer is attached (Fig. 2b). Through the operations of the *c*-glide plane at (*x*, 0, *z*), *t* at (1/2, 1/2, 0), and 2-fold screw axis at (1/4, 1/4, *z*) (Fig. 1c), such

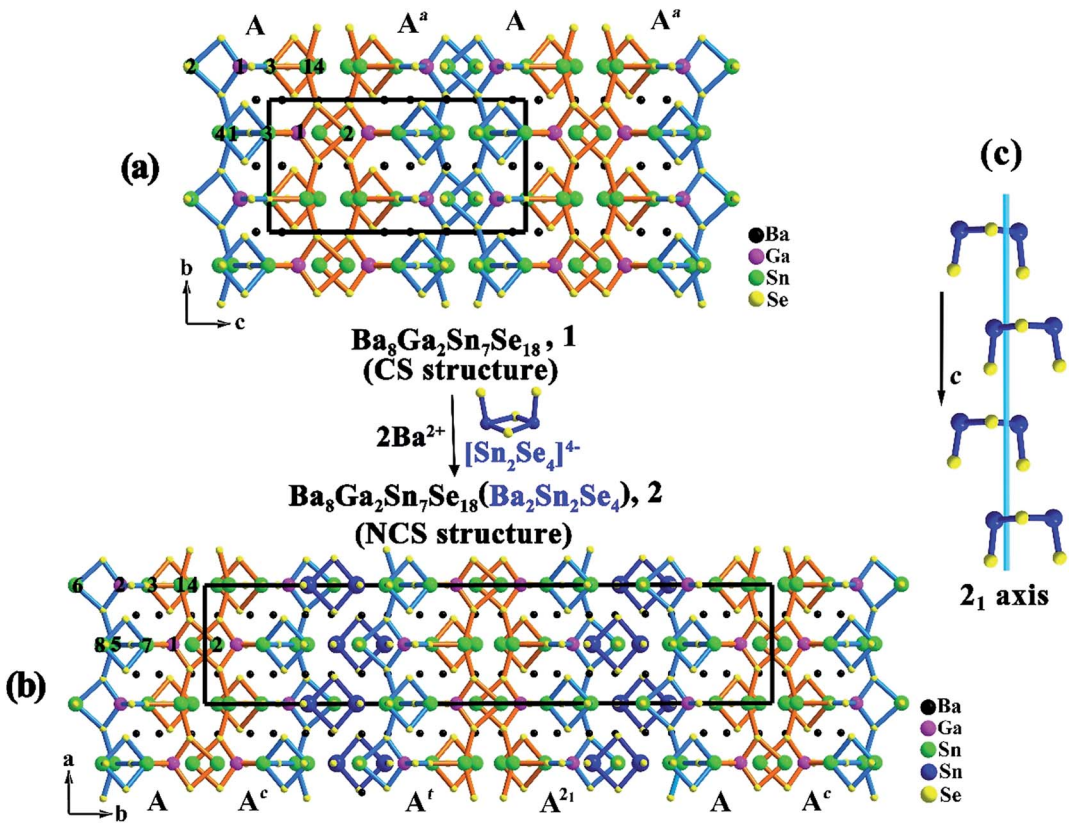

Fig. 1 The packing of the ladder chain in (a) $Ba_8Ga_2Sn_7Se_{18}$, **1** with a sequence of …AA^a…; and (b) $Ba_{10}Ga_2Sn_9Se_{22}$, **2** with a sequence of …AA^{c}A^{t}A^{21}….; every two ladder chains in **2** are separated by isolated $[Sn_2Se_4]$ units (dark blue). The asymmetric unit of the ladder chain is marked by atom numbers. Each ladder chain is combined by Chain 1 (orange) and Chain 2 (blue) *via* sharing of common Se atoms. (c) The $[Sn_2Se_4]$ units in **2** viewed from *a* direction, and 2_1 screw axis at (1/4, 1/4, *z*) is visualized as a light blue line.

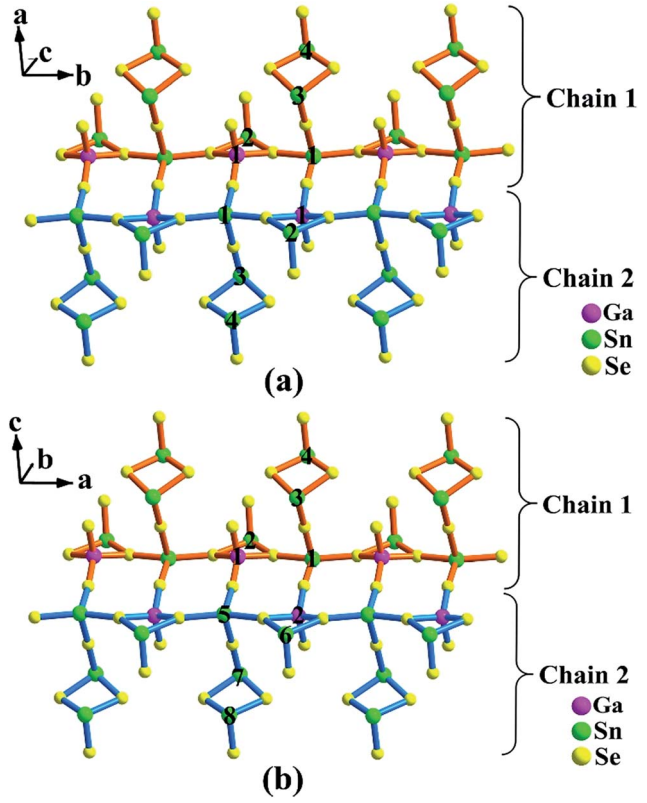

Fig. 2 A single ladder chain in $Ba_8Ga_2Sn_7Se_{18}$, **1** (a); and $Ba_{10}Ga_2Sn_9Se_{22}$, **2** (b). The Ga, Sn atoms are marked with atom numbers.

a ladder chain is thus packed in a sequence of …$AA^cA^tA^{21}$… along the *b* direction (Fig. 1b). In short, the major structure difference between **1** and **2** lies in that the latter contains a matrix of isolated dimeric [Sn(9)Sn(10)Se_4] units (ESI Fig. S7†).

All the Ba atoms are 7-fold coordinated in monocapped trigonal prism geometries with normal Ba–Se bonds ranging from 3.257 (2) to 3.677 (2) Å (ESI Fig. S8†). The Ga–Se distances are normal, varying from 2.382 (3) to 2.424 (2) Å. The 3-fold coordinated Sn atoms (Sn = Sn(2)–(4), (6)–(10)) have regular Sn–Se bond lengths ranging from 2.581 (3) to 2.920 (2) Å. Similar as in **1**, Sn(1) and Sn(5) atoms (with 50% occupancies) are 4-fold coordinated with 3 short Sn–Se bond lengths about 2.83 Å and 1 long bond about 2.95 Å (ESI Fig. S9†). The calculated BVS of Sn(1) and Sn(5) are 1.916 and 1.894, respectively, which demonstrates that the oxidation state of Sn(1) and Sn(5) should be 2+. Selected bond distances are listed in ESI Table S2b.†

Structure relationship

The two short unit cell parameters in $Ba_8Ga_2Sn_7Se_{18}$, **1** and $Ba_{10}Ga_2Sn_9Se_{22}$, **2**, are almost the same (a = 12.466 (9) Å, b = 9.358 (6) Å for **1** *vs.* a = 9.384 (2) Å, c = 12.416 (2) Å for **2**) (Table 1), because the motifs of the ladder chains in both **1** and **2** are nearly identical. Only the packing of the ladder chains is different, that is in **2**, every two of the ladder chains are separated by the isolated dimeric [Sn_2Se_4] units, which leads to the expansion of the long axis. This also generates a chemical formula relationship of $Ba_8Ga_2Sn_7Se_{18}$ (**1**) + $Ba_2Sn_2Se_4$ = $Ba_{10}Ga_2Sn_9Se_{22}$ (**2**). The theoretical formation energy calculations below reveal that the energies at the left- and right-hand sides of such an equation are comparable, suggesting a feasible transformation from **1** to **2**. The isolated dimeric [Sn_2Se_4] units in **2** exhibit the point group C_{2v} symmetry. Thus, the involvement of such an asymmetric unit lowers the point group D_{2h} symmetry of **1** *via* the absence of the symmetry elements of n (1/4, y, z), 2_1 (1/4, 0, z), 2_1 (0, y, 0), and center of symmetry. As shown in Fig. 1b, the insertion of isolated [Sn_2Se_4] units between the light blue Chain 2 leads to the symmetry breaking. As a result, each Chain 2 undergoes a slight distortion. For instance, Se(17)–Sn(8)–Se(4) = 94.8° in **2** *vs.* Se(1)–Sn(4)–Se(4) = 97.8° in **1**, and the average bonds of Sn(3)–Se = 2.79 Å, Sn(4)–Se = 2.68 Å in **1** vary within 0.4% in comparison with the corresponding Sn(7)–Se = 2.78 Å, Sn(8)–Se = 2.72 Å in **2**. (ESI Tables S2 and S3†).

As detailed above, the packing sequence of **2** (…$AA^cA^tA^{21}$…along the *b* direction) differs from that of **1** (…AA^a… along the *c* direction), giving rise to enlargement about two times of b = 44.834 (6) Å in **2** with respect to c = 18.14 (2) Å in **1**, because that the embedding of the [Sn_2Se_4] dimers separate every two ladder chains. These two structures directly describe that a centrosymmetric structure (**1**) is transformed to a non-centrosymmetric structure (**2**) by the introduction of the second building unit. These substantially support the commonly applied strategy of "*diversity of the asymmetric unit would enhance the difficulty of spontaneously producing a mirror plane or inversion center during the packing process, an approach involving two or more types of asymmetric building units in a structure would have a high possibility to form a noncentrosymmetric structure*".[15] Many other systems are worth exploring to see if the similar phenomenon exists.

Thermal analyses

The thermogravimetric (TG) curves of compounds **1** and **2** are shown in ESI Fig. S10a and b.† The data results indicate that both of the compounds are stable up to 800 °C under a N_2 atmosphere. In order to further check the thermal stability of the two compounds, pure **1** and **2** were sealed in silica tubes under vacuum and annealed for 3 h at 850 °C respectively. After such a treatment, the X-ray powder diffraction patterns of two compounds showed obvious impurities, which indicated the decomposition of two occurred at around 800 °C (Fig. S10c and d in the ESI†).

UV-Vis-near-IR and IR spectra

The optical band gaps of **1** and **2** are approximately 1.65 and 1.67 eV, respectively, which are in agreement with their black color (Fig. 3). These values are similar to that of $Ba_6Sn_6Se_{13}$ (1.52 eV),[35] in which Sn cations have the mixed oxidation states of 2+ and 4+, but smaller than those of $Ba_4Ga_4SnSe_{12}$ (2.16 eV),[28] $Ba_6Ga_2SnSe_{11}$ (1.99 eV),[28] and $BaGa_2SnSe_6$ (1.95 eV),[29] in which the oxidation state of Sn is 4+. Thus, in Ba/Ga/Sn/Se system, compounds containing Sn^{2+} or mixed valences (Sn^{2+} and Sn^{4+}) have smaller band gaps than those merely containing Sn^{4+}. The IR spectra and UV-Vis-near-IR spectra of **2** show the transparent

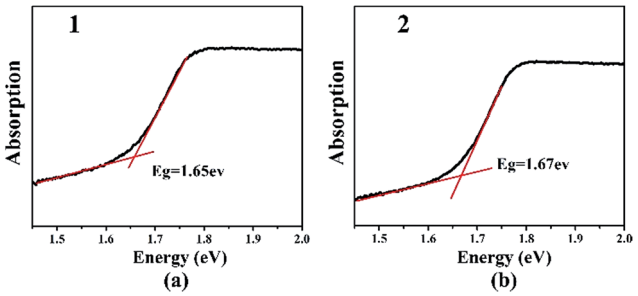

Fig. 3 UV-Vis diffuse reflection spectra of $Ba_8Ga_2Sn_7Se_{18}$, **1** (a) and $Ba_{10}Ga_2Sn_9Se_{22}$, **2** (b).

range roughly from 0.80 to 25 μm, which is comparable with that of the benchmark $AgGaS_2$ (0.15–23 μm, ESI Fig. S11 and S12†).

Second harmonic generation (SHG) property

The SHG of **2** was measured with the 1064 nm and 2050 nm laser radiation as the fundamental wavelength. Unfortunately, no obvious SHG signal was observed. The possible reason might be related to the poor crystallinity of this compound, longer fundamental wavelength should be tried, however, wavelength longer than 2050 nm is not available at present.

Electronic structures

The electronic band structures of **1** and **2** (Fig. 4) reveal the indirect band gaps of 0.83 and 0.88 eV, respectively. Those are smaller than the experimental values (1.65 and 1.67 eV) because of the inaccurate description of the eigenvalues of the electronic states for GGA. The total and partial densities of states (DOS and PDOS) of **1** and **2** are given in Fig. 5. Take **1** as an example, the valence band (VB) between −9 and −5 eV contains Ga-4s and Sn-5s states with minor Se-4p and Se-4s states. The VB from −5 to −2 eV is mainly composed of Ga-4p, Sn-5p, and Se-4p states. The VB top predominantly originates from Se-4p, and minor Ga-4p, Sn-5s, and Sn-5p states. Above the Fermi level, the bottom of the conduction band (CB) is dominated by Sn-5p, and Se-4p

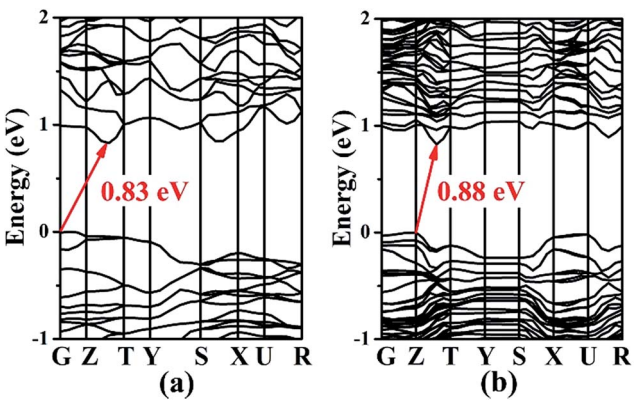

Fig. 4 Calculated band structures of $Ba_8Ga_2Sn_7Se_{18}$, **1** (a) and $Ba_{10}Ga_2Sn_9Se_{22}$, **2** (b).

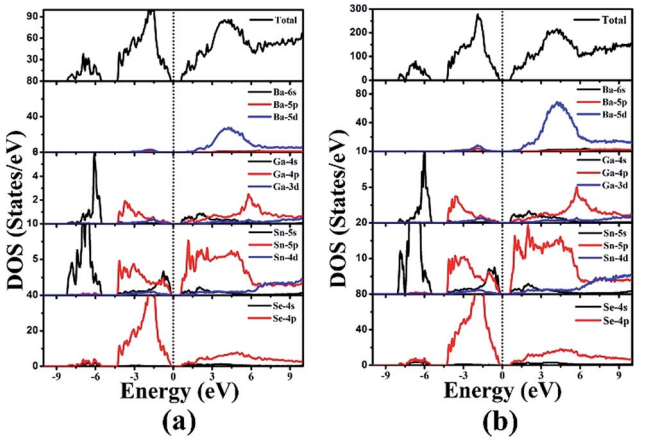

Fig. 5 Total and partial densities of states of $Ba_8Ga_2Sn_7Se_{18}$, **1** (a) and $Ba_{10}Ga_2Sn_9Se_{22}$, **2** (b).

states mixed with a small amount of Ga-4s, Ga-4p, and Sn-5s states. The CB ranging from 2 to 5 eV is composed of Ba-5d, Ga-4p, Sn-5p, and Se-4p states. Thus, the band gap absorption is mainly ascribed to the charge transitions from Se-4p to Sn-5p states. By comparing the PDOS of Sn^{2+} (for **1** and **2**) and Sn^{4+} (for $Ba_4Ga_4SnSe_{12}$,[28] $Ba_6Ga_2SnSe_{11}$,[28] and $BaGa_2SnSe_6$ (ref. 29)) near the Fermi surface, we find that the Sn-5s state of Sn^{4+} has no obvious peak at the VB top, while for Sn^{2+}, an obvious contribution of Sn-5s state appears at the VB top, which narrows the band gap. As a result, compounds containing Sn^{2+} or mixed valences (Sn^{2+} and Sn^{4+}) have smaller band gaps than those containing Sn^{4+}. This is in good accordance with the experimental results (1.65 and 1.67 eV for **1** and **2**; 2.16, 1.99, and 1.95 eV for $Ba_4Ga_4SnSe_{12}$,[28] $Ba_6Ga_2SnSe_{11}$,[28] and $BaGa_2SnSe_6$,[29] respectively).

Energies calculation

The formation energies with respect to the isolated atoms of compounds **1**, **2** and $BaSnSe_2$ were calculated by the following equation:

$$E_f = \frac{E_t - n_{Ba}E_{Ba} - n_{Ga}E_{Ga} - n_{Sn}E_{Sn} - n_{Se}E_{Se}}{n_{Ba} + n_{Ga} + n_{Sn} + n_{Se}}$$

where E_f is the formation energy and E_t is the total energy of a compound.

Compounds **1** and **2** have the following chemical formula relationship:

$$Ba_8Ga_2Sn_7Se_{18}\ (\mathbf{1}) + 2BaSnSe_2 = Ba_{10}Ga_2Sn_9Se_{22}\ (\mathbf{2})$$

And the energy of the combination reaction can be defined as

$$E = E_f(Ba_{10}Ga_2Sn_9Se_{22}) - E_f(Ba_8Ga_2Sn_7Se_{18}) - E_f(Ba_2Sn_2Se_4)$$

The calculated energy of the combination reaction is −1.28 eV indicating that the noncentrosymmetric $Ba_{10}Ga_2Sn_9Se_{22}$ is

slightly energetically favorable. Hence, the transformation from centrosymmetric **1** to noncentrosymmetric **2** is feasible.

Conclusion

In summary, two new selenides with their own structure types, centrosymmetric $Ba_8Ga_2Sn_7Se_{18}$, **1** and noncentrosymmetric $Ba_{10}Ga_2Sn_9Se_{22}$, **2**, have been discovered by solid-state reactions. Both structures feature 1D ladder chain built by alternatively jointed $GaSe_4$ tetrahedron and $SnSe_4$ tetragonal pyramid. To each of these polyhedra, an accessory, $SnSe_3$ pyramid or Sn_2Se_4 dimer, is attached. Interestingly, the structure of **2** is the combination of that of **1** and the isolated $[Sn_2Se_4]$ dimer with a C_{2v} symmetry. The embedding of the asymmetric dimeric $[Sn_2Se_4]$ in **2** vanishes the operations of n, 2_1, and the center of symmetry that exist in **1**. Significantly, **1** and **2** directly describe for the first time that a centrosymmetric-to-noncentrosymmetric structure transformation is caused by a simple combination reaction. This work supports the commonly applied strategy of "*involving two or more types of asymmetric building units in a structure would have a high possibility to form a noncentrosymmetric structure*".[15] This insight will shed useful light on the future exploration of new NCS materials.

Acknowledgements

This work was supported by the National Natural Science Foundation of China under Projects 21233009, 21225104, 91422303, 21301175, 21571020 and 21671023.

Notes and references

1 (*a*) X. T. Wu and L. Chen, *Structure–Property Relationships in Non-Linear Optical Crystals. I. The UV-Vis Region*, Springer, Berlin, 2012, p. 144; (*b*) X. T. Wu and L. Chen, *Structure–Property Relationships in Non-Linear Optical Crystals. II. The IR Region*, Springer, Berlin, 2012, p. 145.
2 I. Chung and M. G. Kanatzidis, *Chem. Mater.*, 2014, **26**, 849–869.
3 (*a*) H. Lin, L. Chen, L. J. Zhou and L. M. Wu, *J. Am. Chem. Soc.*, 2013, **135**, 12914–12921; (*b*) Y. Y. Li, P. F. Liu, L. Hu, L. Chen, H. Lin, L. J. Zhou and L. M. Wu, *Adv. Opt. Mater.*, 2015, **3**, 957–966; (*c*) Y. Y. Li, P. F. Liu, H. Lin, M. T. Wang and L. Chen, *Inorg. Chem. Front.*, 2016, **3**, 952–958.
4 (*a*) P. Yu, L. M. Wu and L. Chen, *Inorg. Chem.*, 2013, **52**, 724–728; (*b*) A. H. Fang, F. Q. Huang, X. M. Xie and M. H. Jiang, *J. Am. Chem. Soc.*, 2010, **132**, 3260–3261.
5 P. F. P. Poudeu, N. Takas, C. Anglin, J. Eastwood and A. Rivera, *J. Am. Chem. Soc.*, 2010, **132**, 5751–5760.
6 D. Y. Chung, T. Hogan, P. Brazis, M. Rocci-Lane, C. Kannewurf, M. Bastea, C. Uher and M. G. Kanatzidis, *Science*, 2000, **287**, 1024–1027.
7 Z. S. Lin, L. Chen, L. M. Wang, J. T. Zhao and L. M. Wu, *Adv. Mater.*, 2013, **25**, 4800–4806.
8 Y. Hotta, E. Rokuta, J.-H. Jhoi, H. Tabata, H. Kobayashi and T. Kawai, *Appl. Phys. Lett.*, 2002, **80**, 3180–3182.
9 L. Benguigui, R. Weil, E. Muranevich, A. Chack, E. Fredj and A. Zunger, *J. Appl. Phys.*, 1993, **74**, 513–520.
10 B. Scott, M. Pressprich, R. D. Willet and D. A. Cleary, *J. Solid State Chem.*, 1992, **96**, 294–300.
11 I. V. Kityk, N. AlZayed, P. Rakus, A. A. AlOtaibe, A. M. El-Naggar and O. V. Parasyuk, *Phys. B*, 2013, **423**, 60–63.
12 W. Kuznik, P. Rakus, K. Ozga, O. V. Parasyuk, A. O. Fedorchuk, L. V. Piskach, A. Krymus and I. V. Kityk, *Eur. Phys. J.: Appl. Phys.*, 2015, **70**, 30501.
13 B. Lagoun, T. Bentria and B. Bentria, *Comput. Mater. Sci.*, 2013, **68**, 379–383.
14 L. Iordanidis, D. Bilc, S. D. Mahanti and M. G. Kanatzidis, *J. Am. Chem. Soc.*, 2003, **125**, 13741–13752.
15 M. C. Chen, L. M. Wu, H. Lin, L. J. Zhou and L. Chen, *J. Am. Chem. Soc.*, 2012, **134**, 6058–6060.
16 Y. Y. Li, B. X. Li, G. Zhang, L. J. Zhou, H. Lin, J. N. Shen, C. Y. Zhang, L. Chen and L. M. Wu, *Inorg. Chem.*, 2015, **54**, 4761–4767.
17 L. Geng, W. D. Cheng, C. S. Lin, W. L. Zhang, H. Zhang and Z. Z. He, *Inorg. Chem.*, 2011, **50**, 5679–5686.
18 W. L. Yin, W. D. Wang, L. Bai, K. Feng, Y. G. Shi, W. Y. Hao, J. Y. Yao and Y. C. Wu, *Inorg. Chem.*, 2012, **51**, 11736–11744.
19 (*a*) X. S. Lin, G. Zhang and N. Ye, *Cryst. Growth Des.*, 2009, **9**, 1186–1189; (*b*) J. Y. Yao, D. J. Mei, L. Bai, Z. S. Lin, W. L. Yin, P. Z. Fu and Y. C. Wu, *Inorg. Chem.*, 2010, **49**, 9212–9216.
20 X. S. Lin, Y. F. Guo and N. Ye, *J. Solid State Chem.*, 2012, **195**, 172–177.
21 Y. Kim, I. S. Seo, S. W. Martin, J. Baek, P. S. Halasyamani, N. Arumugam and H. Steinfink, *Chem. Mater.*, 2008, **20**, 6048–6052.
22 H. Lin, L. J. Zhou and L. Chen, *Chem. Mater.*, 2012, **24**, 3406–3414.
23 B. W. Liu, H. Y. Zeng, M. J. Zhang, Y. H. Fan, G. C. Guo, J. S. Huang and Z. C. Dong, *Inorg. Chem.*, 2015, **54**, 976–981.
24 M. C. Chen, L. H. Li, Y. B. Chen and L. Chen, *J. Am. Chem. Soc.*, 2011, **133**, 4617–4624.
25 Z. Z. Luo, C. S. Lin, H. H. Cui, W. L. Zhang, H. Zhang, Z. Z. He and W. D. Cheng, *Chem. Mater.*, 2014, **26**, 2743–2749.
26 Z. Z. Luo, C. S. Lin, W. L. Zhang, H. Zhang, Z. Z. He and W. D. Cheng, *Chem. Mater.*, 2014, **26**, 1093–1099.
27 Z. Z. Luo, C. S. Lin, W. D. Cheng, H. Zhang, W. L. Zhang and Z. Z. He, *Inorg. Chem.*, 2013, **52**, 273–279.
28 W. L. Yin, Z. H. Lin, L. Kang, B. Kang, J. G. Deng, Z. S. Lin, J. Y. Yao and Y. C. Wu, *Dalton Trans.*, 2015, **44**, 2259–2266.
29 X. S. Li, C. Li, P. F. Gong, Z. S. Lin, J. Y. Yao and Y. C. Wu, *J. Mater. Chem. C*, 2015, **3**, 10998–11004.
30 L. M. Wu, R. Sharma and D. K. Seo, *Inorg. Chem.*, 2003, **42**, 5798–5800.
31 L. M. Wu and D. K. Seo, *J. Am. Chem. Soc.*, 2004, **126**, 4676–4681.
32 Y. Z. Huang, L. Chen and L. M. Wu, *Cryst. Growth Des.*, 2008, **8**, 739–743.
33 Y. Z. Huang, L. Chen and L. M. Wu, *Inorg. Chem.*, 2008, **47**, 10723–10728.
34 Y. Z. Huang, L. M. Wu, S. W. Du and L. Chen, *Inorg. Chem.*, 2009, **48**, 3901–3903.

35 K. Feng, X. X. Jiang, L. Kang, W. L. Yin, W. Y. Hao, Z. S. Lin, J. Y. Yao, Y. C. Wu and C. T. Chen, *Dalton Trans.*, 2013, **42**, 13635–13641.
36 D. J. Mei, W. L. Yin, Z. S. Lin, R. He, J. Y. Yao, P. Z. Fu and Y. C. Wu, *J. Alloys Compd.*, 2011, **509**, 2981–2985.
37 G. M. Sheldrick, *SHELXTL, version 5.1*. Bruker-AXS: Madison, WI, 1998.
38 A. L. Spek, *J. Appl. Crystallogr.*, 2003, **36**, 7–13.
39 C. L. Teske, *Z. Anorg. Allg. Chem.*, 1978, **445**, 196–201.
40 G. Kortüm, *Reflectance Spectroscopy*; Springer-Verlag: 1969.
41 S. K. Kurtz and T. T. Perry, *J. Appl. Phys.*, 1968, **39**, 3798–3813.
42 G. Kresse and J. Furthmüller, *Phys. Rev. B: Condens. Matter Mater. Phys.*, 1996, **54**, 11169–11186.
43 G. Kresse and D. Joubert, *Phys. Rev. B: Condens. Matter Mater. Phys.*, 1999, **59**, 1758–1775.
44 P. E. Blöchl, *Phys. Rev. B: Condens. Matter Mater. Phys.*, 1994, **50**, 17953–17979.
45 J. E. Iglesias and H. Steinfink, *Acta Crystallogr., Sect. B: Struct. Crystallogr. Cryst. Chem.*, 1973, **29**, 1480–1483.
46 W. L. Yin, K. Feng, W. D. Wang, Y. G. Shi, W. Y. Hao, J. Y. Yao and Y. C. Wu, *Inorg. Chem.*, 2012, **51**, 6860–6867.
47 I. D. Brown and D. Altermatt, *Acta Crystallogr., Sect. B: Struct. Sci.*, 1985, **41**, 244–247.
48 K. O. Klepp and F. Z. Fabian, *Naturforscher*, 1992, **47**, 406–410.
49 A. Assoud, N. Soheilnia and H. Kleinke, *Chem. Mater.*, 2004, **16**, 2215–2221.